Manuscript Details

Manuscript number	COST_2018_1110
Title	Time-dependent assessment and deflection prediction of prestressed concrete beams with unbonded CFRP tendons
Article type	Full Length Article

Abstract

This paper presents the assessment of the time-dependent behavior and the prediction of the long-term deflection of concrete beams prestressed with internal unbonded carbon fiber reinforced polymer (CFRP) tendons. A numerical model for the time-dependent analysis of concrete beams prestressed with unbonded tendons is calibrated against experimental results. Parametric numerical simulations are then conducted on simply supported unbonded prestressed concrete beams subjected to long-term sustained loads to investigate the effect of using CFRP tendons instead of low-relaxation steel ones, the magnitude of the initial prestress, the loading conditions, and the quantity of the compressive reinforcing steel. The results show that the long-term prestress loss of beams with CFRP tendons is considerably higher than that of beams with steel tendons. Moreover, it is shown that increasing the quantity of compressive reinforcing steel leads to a substantial decrease in long-term downward deflection. A modification of the ACI 318-14 equation is proposed to predict the time-dependent deflection of prestressed concrete beams with unbonded FRP or steel tendons.

Keywords	Carbon fiber; Time-dependent behavior; Unbonded tendons; Beams

Corresponding Author	Tiejiong Lou
Corresponding Author's Institution	University of Southampton
Order of Authors	Tiejiong Lou, Theodore Karavasilis
Suggested reviewers	Mantas Atutis, Joaquim Barros

Submission Files Included in this PDF

File Name [File Type]

Cover_letter.doc [Cover Letter]

Manuscript v4.doc [Manuscript File]

To view all the submission files, including those not included in the PDF, click on the manuscript title on your EVISE Homepage, then click 'Download zip file'.

Tiejiong Lou
Faculty of Engineering and the Environment
University of Southampton
SO17 1BJ Southampton
United Kingdom

E-mail: T.Lou@soton.ac.uk

Southampton, 27-March-2018

Editor
Composite Structures
ELSEVIER

Dear Editor,

Please find attached manuscript titled “Time-dependent assessment and deflection prediction of prestressed concrete beams with unbonded CFRP tendons” by Tiejiong Lou and Theodore L. Karavasilis. We would like to have this manuscript reviewed for possible publication in Composite Structures. This manuscript is of original material, i.e. it has not been submitted elsewhere for publication or published elsewhere.
Should you need to contact me, please use the above address. You may also contact me via email at T.Lou@soton.ac.uk.

I look forward to hearing from you.

Yours faithfully,

_____

Dr. Tiejiong Lou
University of Southampton

Time-dependent assessment and deflection prediction of prestressed concrete beams with unbonded CFRP tendons

Tiejiong Lou*[1,2] and Theodore L. Karavasilis[2]

1. Hubei Key Laboratory of Roadway Bridge & Structure Engineering, Wuhan University of Technology, 430070 Wuhan, China
2. Faculty of Engineering and the Environment, University of Southampton, SO17 1BJ Southampton, United Kingdom

Abstract: This paper presents the assessment of the time-dependent behavior and the prediction of the long-term deflection of concrete beams prestressed with internal unbonded carbon fiber reinforced polymer (CFRP) tendons. A numerical model for the time-dependent analysis of concrete beams prestressed with unbonded tendons is calibrated against experimental results. Parametric numerical simulations are then conducted on simply supported unbonded prestressed concrete beams subjected to long-term sustained loads to investigate the effect of using CFRP tendons instead of low-relaxation steel ones, the magnitude of the initial prestress, the loading conditions, and the quantity of the compressive reinforcing steel. The results show that the long-term prestress loss of beams with CFRP tendons is considerably higher than that of beams with steel tendons. Moreover, it is shown that increasing the quantity of compressive reinforcing steel leads to a substantial decrease in long-term downward deflection. A modification of the ACI 318-14 equation is proposed to predict the time-dependent deflection of prestressed concrete beams with unbonded FRP or steel tendons.

Keywords: Carbon fiber; Time-dependent behavior; Unbonded tendons; Beams

* Corresponding author.
E-mail address: T.Lou@soton.ac.uk (T. Lou), T.Karavasilis@soton.ac.uk (T.L. Karavasilis).

1. Introduction

Unbonded tendons have been extensively used for the design or retrofit of concrete members, such as beams and slabs, due to their fast installation and easy replacement. Fiber reinforced polymer (FRP) tendons are recognized as a promising alternative to traditional steel tendons [1]. Glass fibers are generally not recommended for prestressing applications because of creep rupture at a low sustained stress. Aramid and carbon fiber reinforced polymers (AFRP and CFRP) can sustain high stresses, and thus, they are both recommended for prestressing tendons [1]. The effect of bond between FRP tendons and concrete on the flexural behavior of FRP prestressed concrete beams was found to be rather important [2]. Bonded FRP tendons may lead to rupture failure of the beams [3,4], while the use of unbonded tendons is an effective and economical solution to prevent FRP rupture [5]. Extensive studies have been conducted to assess the short-term behavior of concrete beams with internal [5-8] or external [9-13] unbonded FRP tendons.

The mechanical properties of prestressed concrete beams degrade with time as a consequence of time-dependent effects, especially when FRP tendons are used since their relaxation is rather pronounced [14,15]. Therefore, a rigorous time-dependent evaluation of FRP tendon systems would be of practical importance. While a great number of works have been conducted to evaluate the long-term behavior of prestressed concrete beams with steel tendons [16-20], there are relatively few studies on the time-dependent assessment of prestressed concrete beams with FRP tendons. Pisani [21,22] proposed both general and simplified approaches for the time-

dependent analysis of concrete beams with bonded AFRP tendons. Lou et al. [23] examined the long-term behavior of concrete beams with bonded AFRP tendons using the finite element method. The latter work also compared the long-term performance when either AFRP or steel tendons were used. Youakim and Karbhari [24] performed a comparative study on the time-dependent behavior of prestressed concrete beams using either FRP or steel tendons. However, the relaxation of CFRP tendons was neglected in their study. All the previously mentioned studies were focused on bonded AFRP tendons. Therefore, there is an apparent need for the assessment of the long-term behavior and the quantification of the prestress loss of concrete beams with unbonded CFRP tendons.

The deflection control at long-term sustained loads is an important task for designers so as to meet the serviceability requirement. It is necessary to develop a simplified equation for calculating the long-term deflection of prestressed concrete beams with unbonded FRP tendons for design purposes. ACI 318-14 [25] recommends an equation which adopts the compressive reinforcement ratio as a key parameter for predicting the long-term deflection of conventional concrete beams. This equation, however, may not be applied to prestressed concrete beams with FRP or steel tendons as it neglects the prestress-related parameters which may have notable impact on the long-term deflection.

This paper presents a numerical study on the time-dependent performance of concrete beams internally prestressed with unbonded CFRP tendons. A previously developed model [26] for time-dependent analysis of concrete beams with unbonded

steel tendons is extended to capture the time-dependent behavior when CFRP tendons are used. The study focuses on the assessment of different parameters including the tendon type, the magnitude of the initial prestress, the load conditions, and the quantity of compressive reinforcing steel. A modification of the ACI 318-14 equation is proposed for calculating the time-dependent deflection of prestressed concrete beams with unbonded FRP or steel tendons.

2. Beam element

The proposed beam element is developed on the basis of specific assumptions, namely, a complete bond between reinforcing steel and concrete is assumed and beam shear deformations are neglected. Consider the local coordinate system (x, y) of a plane beam element defined by two end nodes, as shown in Fig. 1. The element nodal displacements can be conveniently written as $\boldsymbol{r}^e = \{\boldsymbol{u}^T, \boldsymbol{v}^T, \boldsymbol{\theta}^T\}^T$, in which $\boldsymbol{u} = \{u_i, u_j\}^T$, $\boldsymbol{v} = \{v_i, v_j\}^T$ and $\boldsymbol{\theta} = \{\theta_i, \theta_j\}^T$ represent nodal axial displacements, transverse displacements, and rotations, respectively. By assuming a linear variation of the axial displacement u and a cubic variation of the transverse displacement v along the beam longitudinal axis, both displacements can be mathematically expressed as $u = \boldsymbol{N}_1\boldsymbol{u}$ and $v = \boldsymbol{N}_2\{\boldsymbol{v}^T, \boldsymbol{\theta}^T\}^T$, in which $\boldsymbol{N}_1 = [1–p, p]$ and $\boldsymbol{N}_2 = [1–3p^2+2p^3, 3p^2–2p^3, l(p–2p^2+p^3), l(–p^2+p^3)]$. In the latter expression, p is equal to x/l, where l is the length of the element.

By assuming that the nonmechanical strain in concrete consists of creep and shrinkage strains, the increase in concrete stress $\Delta\sigma_c$ within a time interval can be

expressed as $\Delta\sigma_c = E_c\Delta\varepsilon_c^m = E_c(\Delta\varepsilon_c - \Delta\varepsilon_c^{cr} - \Delta\varepsilon_c^{sh})$, in which E_c is the tangential modulus of concrete; and $\Delta\varepsilon_c$, $\Delta\varepsilon_c^m$, $\Delta\varepsilon_c^{cr}$ and $\Delta\varepsilon_c^{sh}$ are the increases in total, mechanical, creep and shrinkage strains in concrete, respectively. At service condition, the creep strain of concrete at time *t* may be evaluated by

$$\varepsilon_c^{cr}(t) = \sigma_c(t_0)C(t,t_0) + \int_{t_0}^{t} C(t,\tau)\frac{\partial\sigma_c(\tau)}{\partial\tau}d\tau \tag{1}$$

$$C(t,\tau) = \sum_{k=1}^{m}\phi_k(\tau)[1-e^{-r_k(t-\tau)}] \tag{2}$$

in which $\sigma_c(t_0)$ is the initial stress at age t_0; $\sigma_c(\tau)$ is the stress at age τ; and *m*, $\phi_k(\tau)$ and r_k are coefficients. The Dirichlet series creep function, proposed by Zienkiewicz and Watson [27] and represented by Eq. (2), has been widely adopted by investigators [20,28,29] for the creep analysis of concrete structures due to its effectiveness in simulating the stress history. On the other hand, the shrinkage strain of concrete may be calculated as [30]: $\varepsilon_c^{sh}(t) = \varepsilon_{cs0}t/(35+t)$ where ε_{cs0} is the notional total drying shrinkage.

By applying the principle of virtual work, the following time-dependent incremental governing equations for an element can be established [26]:

$$\Delta\boldsymbol{R}^e + (\Delta\boldsymbol{R}^e)^{cr} + (\Delta\boldsymbol{R}^e)^{sh} = (\boldsymbol{K}_o^e + \boldsymbol{K}_g^e)\Delta\boldsymbol{r}^e \tag{3}$$

where

$$(\Delta\boldsymbol{R}^e)^{cr} = \int_{V1}\boldsymbol{B}^T E_c\Delta\varepsilon_c^{cr}d(V1), \quad (\Delta\boldsymbol{R}^e)^{sh} = \int_{V1}\boldsymbol{B}^T E_c d(V1)\Delta\varepsilon_c^{sh} \tag{4}$$

$$\boldsymbol{K}_o^e = \int_V \boldsymbol{B}^T E\boldsymbol{B}dV, \quad \boldsymbol{K}_g^e = \int_V \sigma\boldsymbol{J}^T\boldsymbol{J}dV \tag{5}$$

$$\boldsymbol{B} = \left[\frac{d\boldsymbol{N}_1}{dx} \quad -y\frac{d^2\boldsymbol{N}_2}{dx^2}\right], \quad \boldsymbol{J} = \left[0 \quad 0 \quad \frac{d\boldsymbol{N}_2}{dx}\right] \tag{6}$$

in which $\Delta\boldsymbol{R}^e$ are the equivalent nodal load increments due to external loads and

unbonded prestressing; $(\Delta \boldsymbol{R}^e)^{cr}$ and $(\Delta \boldsymbol{R}^e)^{sh}$ are the equivalent nodal load increments due to concrete creep and shrinkage, respectively; $\Delta \boldsymbol{r}^e$ are the nodal displacement increments; σ is the stress; $V1$ is the concrete volume of each element; and V is the element volume that consists of concrete and its reinforcing steel. The integration described by Eqs. (4) and (5) is carried out by applying a layered technique. The governing equations for the structure are assembled in the global coordinate system (X, Y) and solved by the incremental-iterative method [26].

As shown in Fig. 1, the tendon segment is considered to be straight and its length is calculated from

$$l_p = \sqrt{(X_{pj} - X_{pi})^2 + (Y_{pj} - Y_{pi})^2} \tag{7}$$

where X_{pi}, Y_{pi}, X_{pj} and Y_{pj} are the global coordinates of the two end joints of the tendon segment. The latter are determined by using the following equations:

$$X_{pi} = X_{pi0} + \overline{u}_i - e_i \overline{\theta}_i \cos\alpha_0, \quad Y_{pi} = Y_{pi0} + \overline{v}_i - e_i \overline{\theta}_i \sin\alpha_0 \tag{8}$$

$$X_{pj} = X_{pj0} + \overline{u}_j - e_j \overline{\theta}_j \cos\alpha_0, \quad Y_{pj} = Y_{pj0} + \overline{v}_j - e_j \overline{\theta}_j \sin\alpha_0 \tag{9}$$

in which X_{pi0}, Y_{pi0}, X_{pj0} and Y_{pj0} are the original global coordinates of the two end joints; e_i and e_j are the eccentricities of the unbonded tendon at the two end nodes; α_0 is the original angle between the global and local coordinate axes; and $\overline{u}_i$, $\overline{v}_i$, $\overline{\theta}_i$, $\overline{u}_j$, $\overline{v}_j$ and $\overline{\theta}_j$ are the displacements and rotations at two end nodes with respect to the global X-Y coordinate system shown in Fig. 1.

The increase in strain in the unbonded tendon can be expressed as: $\Delta\varepsilon_p = (\sum l_p - \sum l_{p0}) / \sum l_{p0}$, where l_{p0} is the original segment length. The tendon strain is then obtained from $\varepsilon_p = \varepsilon_{p0} + \Delta\varepsilon_p$, where ε_{p0} is the initial tendon strain.

The FRP tendon is linearly elastic until rupture, while the steel tendon at service conditions can be considered to be within its elastic range. Therefore, when the tendon relaxation σ_{pr} is considered, at service conditions the stress in the FRP or steel tendons can be calculated as $\sigma_p = \varepsilon_p E_p + \sigma_{pr}$, where E_p is the tendon modulus of elasticity. The equivalent loads due to unbonded prestressing are then easily computed following the procedure in [26].

In this study, the intrinsic relaxation for CFRP tendons is evaluated by the equation recommended by Saadatmanesh and Tannous [14]:

$$\frac{\sigma_{pr}}{\sigma_{p0}} = -\frac{\sigma_{p0}/\sigma_{pu} - [a - b\log(\tau - t_0)]}{\sigma_{p0}/\sigma_{pu}} \tag{10}$$

where $(\tau - t_0)$ is the relaxation time in hours; σ_{p0} is the initial tendon stress for relaxation; σ_{pu} is the tendon ultimate tensile strength; and a and b are coefficients. For Leadline tendons in air at temperature of 25°C, a is equal to 0.3846 and b is equal to 0.0046 at 40% initial prestress level, while a is equal to 0.5546 and b is equal to 0.0063 at 60% initial prestress level [14].

The intrinsic relaxation for low-relaxation steel tendons is evaluated by [31]

$$\frac{\sigma_{pr}}{\sigma_{p0}} = -\frac{\log(\tau - t_0)}{30}\left(\frac{\sigma_{p0}}{f_{py}} - 0.55\right) \tag{11}$$

in which f_{py} is the steel tendon yield stress.

3. Comparison of numerical predictions with experimental data

Breckenridge and Bugg [32] performed detailed long-term tests on simply supported prestressed concrete beams under sustained loading of 8 years. Their

specimens include several prestressed concrete beam specimens with unbonded steel tendons. Two of these specimens are identical apart from their loading conditions, i.e. one beam sustained its self-weight load only, while the other one sustained its self-weight and two point loads. The point loads are both equal to 67.6 kN and are applied at distance from the end support equal to one quarter of the beam span as shown in Fig. 2. The material properties for the prestressing steel are E_p = 169 GPa, f_{py} = 896 MPa, and σ_{p0} = 683.8 MPa; for the reinforcing steel E_s = 200 GPa, where E_s is the elastic modulus of reinforcing steel; and for the concrete E_c = 24.1 GPa at 22 days. The value of ε_{cs0} is equal to 366 × 10^{-6}.

Zhu [33] proposed the following creep data for preliminary design of large concrete dams: m = 2, $\phi_1(\tau) = \beta_1(1+9.2\tau^{-0.45})/E_0$, r_1 = 0.3, β_1 = 0.23, $\phi_2(\tau) = \beta_2(1+1.7\tau^{-0.45})/E_0$, r_2 = 0.005, β_2 = 0.52. E_0 is associated with the time-dependent modulus of elasticity, i.e. $E_c(\tau) = E_0(1-e^{-0.4\tau^{0.34}})$. In the present study, the creep data proposed by Zhu [33] are modified, i.e. r_1 = 0.1, β_1 = 0.46 and β_2 = 1.04, in order to capture the time-dependent behavior of the prestresssed concrete beam specimens tested by Breckenridge and Bugg [32]. Using these creep data, the beam element discussed in Section 2 is used to numerically predict the long-term behavior of the prestressed concrete beam specimens. Fig. 2 compares the predicted time-dependent deflections (using the original [33] and the modified creep data) with the experimental ones for a period of 7 years. When the creep data proposed by Zhu [33] are used, the analysis considerably underestimates the long-term deflections. On the other hand, when the modified Zhu data is used in the analysis, the calculated and

experimental values are shown to be in satisfactory agreement. Therefore, the proposed beam element along with the modified concrete creep data is used to conduct the numerical study described in the following sections.

4. Evaluation of long-term behavior

4.1. Beams

A numerical study is conducted to investigate the long-term behavior of concrete beams internally prestressed with unbonded CFRP tendons. The beams have a rectangular cross section (300×600 mm) and are simply supported over a span of 12 m, as shown in Fig. 3(a). The profile of unbonded tendons is assumed to be parabolic. The tendon eccentricities over the end support (e_0) and midspan (e_1) are equal to 0 mm and 200 mm, respectively. The area of the prestressing tendons, A_p, is equal to 10 cm^2, of the tensile reinforcing steel, A_s, is equal to 7.2 cm^2, and of the compressive reinforcing steel, $A_s^{'}$, is equal to 3.6 cm^2. Two load conditions are considered, i.e. self-weight and P = 0 kN (i.e. beams without external loads) or self-weight and P = 100 kN (i.e. beams with service external loads), where P are the third point loads acting on the beams.

The unbonded tendons are made of either CFRP composites or low-relaxation prestressing steel to allow a meaningful comparison to be made. CFRP tendons are assumed to be the same as the Leadline tendon specimens tested by Saadatmanesh and Tannous [14]. The mechanical properties for CFRP and steel tendons are given in Table 1, where ε_{pu} is the tendon ultimate strain. Two initial prestress values are

considered, i.e. 800 MPa and 1200 MPa. The yield strength and elastic modulus of the reinforcing steel are equal to 450 MPa and 200 GPa, respectively. The cylinder compressive strength and elastic modulus of concrete at day 28 (assumed to be the day of prestress transfer and loading) are equal to 35 MPa and 34 GPa, respectively. The finite element model of the beam is illustrated in Fig. 3(b).

4.2. Results and discussion

4.2.1. Long-term behavior due to concrete creep and concrete shrinkage

A numerical analysis neglecting the relaxation of prestressing tendons is conducted first in order to isolate the contribution of concrete creep and shrinkage to the time-dependent behavior. Fig. 4 shows the long-term prestress loss in CFRP and steel tendons caused by concrete creep and shrinkage for unbonded beams with different initial prestress levels and load conditions. Figs. 4(a) and (b) show that the prestress loss initially increases quickly and then slows down with time. For a given tendon type and load condition, a higher initial prestress leads to a significantly higher prestress loss. For a given tendon type and initial prestress, the beam with service external loads experiences a lower prestress loss than that without external loads. Because the elastic modulus of CFRP tendons (149.6 GPa) is lower than that of steel ones (195 GPa), CFRP tendons exhibit considerably lower prestress loss than steel ones when tendon relaxation is ignored in the numerical analysis. The ratio of the long-term prestress loss in CFRP tendons to that in steel ones ($\sigma_{loss}^{CFRP} / \sigma_{loss}^{steel}$) is around 0.8 over time, independently of the initial prestress and load condition, as displayed in Fig. 4(c).

The long-term deflection and stress in bottom reinforcing steel at midspan caused by concrete creep and shrinkage are shown in Fig. 5. It is seen that at zero external loads, as a result of the lower prestress loss, CFRP tendons result in higher long-term camber and higher compressive stress in the bottom reinforcing steel compared to steel ones. Under service loading (P = 100 kN), CFRP tendons lead to lower downward deflection than steel ones, particularly for the case of initial prestress of 800 MPa. Just after the application of external loads, the bottom reinforcing steel is in tension for an initial prestress of 800 MPa, while it is in compression for an initial prestress of 1200 MPa. Due to the effects of concrete creep and shrinkage, the tensile stress (if any) gradually disappears and compressive stress develops. The long-term compressive stress in the bottom reinforcing steel of beams with CFRP tendons is higher than that of beams with steel tendons. The latter observation is more pronounced for the initial prestress of 1200 MPa.

4.2.2. Long-term behavior due to concrete creep, concrete shrinkage and tendon relaxation

Stress relaxation of CFRP tendons is significantly higher than that of steel ones. Fig. 6 shows the long-term prestress loss in CFRP and steel tendons caused by concrete creep, concrete shrinkage and tendon relaxation for beams with different initial prestress levels and load conditions. In particular, as can be observed in Fig. 6(a) and (b), CFRP tendons exhibit much higher prestress loss due to concrete creep, shrinkage and tendon relaxation despite the smaller modulus of elasticity of CFRP composites when compared to steel tendons. It is seen in Fig. 6(c) that the

$\sigma_{loss}^{CFRP} / \sigma_{loss}^{steel}$ ratio decreases quickly as time passes and tends to stabilize several months later. The initial prestress does not affect the $\sigma_{loss}^{CFRP} / \sigma_{loss}^{steel}$ ratio in the case of without external loads, while in the case of external loads of 100 kN, a higher prestress level results in lower $\sigma_{loss}^{CFRP} / \sigma_{loss}^{steel}$ ratio. At a given prestress level, unbonded prestressed concrete beams without external loads exhibit a substantially lower $\sigma_{loss}^{CFRP} / \sigma_{loss}^{steel}$ ratio compared to those with external loads, especially for the initial prestress of 800 MPa.

Fig. 7 shows the long-term deflection and stress in bottom reinforcing steel at midspan caused by concrete creep, shrinkage and tendon relaxation for beams with different initial prestress levels and load conditions. After a long period of time, due to higher prestress loss, CFRP tendons exhibit a lower camber (for P = 0 kN) and a higher downward deflection (for P = 100 kN) compared to steel ones. The development of long-term compressive stress in bottom reinforcing steel of beams with CFRP tendons is slower than that of beams with steel tendons.

4.2.3. Influence of compressive reinforcing steel on long-term behavior

In a previous study by Lou et al. [23], the long-term behavior of simply supported bonded AFRP prestressed concrete beams having various tensile reinforcing bars has been analyzed. That study showed that the tensile reinforcing bars affect heavily the long-term behavior under zero external loads but their effect appears to be less pronounced at a certain level of sustained external loads. The latter conclusion holds true for the prestressed concrete beams with unbonded CFRP tendons investigated in this study; yet the results are not presented herein due to space and length limitations.

In this study, the effect of compressive reinforcing steel ratio (ρ_s') on the time-dependent behavior of simply supported prestressed concrete beams with internal unbonded CFRP tendons is explored. Fig. 8 shows the effect of compressive reinforcing steel ratio on the long-term deformations (i.e. midspan deflection, axial shortening, concrete strains in the bottom and top fibers of the midspan section) for beams without external loads, while the results produced for the case that P = 100 kN are illustrated in Fig. 9. Fig. 8 shows that for the case without external loads, the compressive reinforcing steel influences notably the long-term camber and concrete strain of the top fiber, whereas its influence on the long-term axial shortening and concrete strain in the bottom fiber is negligible. As the compressive reinforcing steel ratio increases, the long-term camber increases while the long-term concrete compressive strain in the top fiber decreases substantially. Moreover, increasing the quantity of compressive reinforcing steel leads to a slight decrease in long-term axial shortening and increase in long-term concrete compressive strain in the bottom fiber.

It has been stated that the presence of reinforcing steel would reduce substantially the long-term camber of prestressed concrete beams [34]. This statement, however, is not fully correct. When the tensile reinforcing steel is provided or its quantity is increased in prestressed concrete beams, the long-term camber is significantly reduced, as confirmed in a recent numerical work [23]. On the other hand, the presence or an increasing amount of compressive reinforcing steel leads to an increase in the long-term camber as mentioned above.

Fig. 9 shows that at sustained service loads (P = 100 kN), the quantity of

compressive reinforcing steel has significant influences on the time-dependent performance. The long-term downward deflection, axial shortening and concrete compressive strain in the top fiber are reduced substantially as the quantity of compressive reinforcing steel increases. At P = 100 kN, the concrete strain in the bottom fiber is in tension for the initial prestress of 800 MPa, while for the initial prestress of 1200 MPa is in compression. Increasing the quantity of compressive reinforcing steel leads to a considerable decrease in long-term concrete tensile strain or increase in long-term concrete compressive strain in the bottom fiber.

5. Proposed equation for calculating the long-term deflection

The effectiveness of adding compressive reinforcing steel in reducing the long-term deflection of concrete members is taken into account in ACI 318-14 [25] through a reduction factor α, i.e.:

$$\alpha = \frac{1}{1+50\rho_s'} \tag{12}$$

At service loads of 100 kN, a comparison between the α values predicted by ACI 318-14 and numerical simulations for unbonded CFRP tendon beams (see Fig. 3) subjected to sustained loading of 12 months is illustrated in Fig. 10. Initial prestress values of 800 MPa (i.e. 40% of the ultimate tensile strength) and 1200 MPa (i.e. 60% of the ultimate tensile strength) are used for the investigation. The results of numerical simulations show that as the initial prestress level increases, the influence of the compressive reinforcing steel increases. It is also apparent that ACI 318-14 underestimates the influence of compressive reinforcing steel on the long-term

deflection of prestressed concrete beams. This underestimation is particularly notable at a high initial prestress level.

In order to extend Eq. (12) to the case of prestressed concrete beams with FRP and steel tendons, the following modification is proposed:

$$\alpha = \frac{1}{1+50\eta_e\eta_p\rho_s'} \tag{13}$$

where

$$\eta_e = \frac{E_s}{E_p} \tag{14}$$

and

$$\eta_p = \begin{cases} 1.0 & \text{for } \dfrac{\sigma_{p0}}{\sigma_{pu}} \le 0.4 \\ 2.5\dfrac{\sigma_{p0}}{\sigma_{pu}} & \text{for } \dfrac{\sigma_{p0}}{\sigma_{pu}} > 0.4 \end{cases} \tag{15}$$

In the above equations, η_p represents the effect of the initial prestress level (ratio of initial prestress to ultimate strength of the tendon material); and η_e represents the effect of the tendon modulus of elasticity. For steel tendons, their elastic modulus can be considered equal to that of reinforcing steel, and therefore, η_e in that case is equal to 1.0. For FRP tendons, the value of η_e depends on the modulus of elasticity of the FRP material.

Fig. 11 illustrates a comparison between the α values predicted by ACI 318-14, the proposed Eq. (13) and numerical simulations for different periods of sustained loading (P = 100 kN) and initial prestress levels in unbonded CFRP tendons. Given an initial prestress level, the difference between the results of numerical simulations for different loading periods is not large, indicating that the reduction factor α is almost

time-independent. It is also seen that the results predicted by the proposed equation are in good agreement with those from numerical simulations. Therefore, the proposed modification of the ACI 318-14 equation by introducing the parameters η_e and η_p appears to be reasonable for calculating the reduction factor α.

An empirical equation is recommended in ACI 318-14 to calculate the long-term deflection of concrete members:

$$\lambda_\Delta = \frac{\xi}{1+50\rho_s'} \tag{16}$$

where λ_Δ is the ratio of the time-dependent deflection to the immediate deflection, while ξ is a time-dependent factor, which is equal to 1.0, 1.2, 1.4 and 2.0 for loading periods of 3 months, 6 months, 12 months and 5 years, respectively.

At service external loads of 100 kN, a comparison between the results predicted by ACI 318-14 and numerical simulations in terms of the variation of λ_Δ with ρ_s' for different loading periods and initial prestress levels is illustrated in Figs. 12 and 13. Fig. 12 shows that for initial prestress of 800 MPa and sustained loading for a period equal to or less than 12 months, ACI 318-14 predicts well the time-dependent deflection of prestressed beams without compressive reinforcing steel. However, ACI 318-14 generally overestimates the time-dependent deflection for prestressed beams with compressive reinforcing steel. For a 5-year duration of loading, ACI 318-14 leads to a considerable overestimation, indicating that the ξ value of 2.0 specified is rather conservative. Fig. 13 shows that for an initial prestress of 1200 MPa, ACI 318-14 substantially overestimates the time-dependent deflection regardless of the duration of loading. Therefore, an extension of Eq. (16) to the case of prestressed

concrete members is deemed necessary. The latter is achieved by using the modified reduction factor in Eq. (13) and by replacing ξ with ξ_p, i.e.:

$$\lambda_{\Delta} = \frac{\xi_p}{1+50\eta_e\eta_p\rho_s^{'}} \tag{17}$$

where

$$\xi_p = \frac{\xi}{\eta_p} \tag{18}$$

A comparison of the predictions obtained from ACI 318-14 Eq. (16), the proposed Eq. (17), and numerical simulations is presented in Figs. 12 and 13. Moreover, the correlation of the predictions of the simplified equations (ACI 318-14 and proposed) and the results from numerical simulations for λ_{Δ} is presented in Fig. 14. A total of 40 prestressed concrete beams with unbonded CFRP tendons are used to produce this correlation. It can be seen in Figs. 12-14 that the predictions of the proposed equation and the results of numerical simulations are generally in good agreement. Moreover, the proposed equation seems to be far more accurate than the ACI 318-14 equation in prediction of the time-dependent deflection of prestressed concrete beams with unbonded tendons.

6. Conclusions

The long-term performance of prestressed concrete beams with unbonded CFRP tendons is investigated by using a time-dependent finite element model. The proposed model is validated against long-tem tests on unbonded prestressed concrete specimens. It is shown that by modifying the creep data recommended by Zhu [33], the proposed

finite element model simulates well the experimental results. Time-dependent assessments are then performed to reveal the effect of using CFRP tendons instead of low-relaxation steel ones, the magnitude of the initial prestress, the loading conditions and the compressive reinforcing steel ratio. Moreover, the empirical equation recommended in ACI 318-14 for calculating the long-term deflection is evaluated, and a modified ACI 318-14 equation is proposed. On the basis of the results presented herein, the following conclusions are drawn:

- The long-term prestress loss due to concrete creep and shrinkage only (i.e. without considering tendon relaxation) in CFRP tendons is about 80% of that in steel tendons. CFRP tendons exhibit higher long-term prestress loss due to concrete creep, shrinkage and tendon relaxation than steel tendons, especially for beams under sustained external loads.
- When only concrete creep and shrinkage are considered, CFRP tendons induce a higher long-term prestress camber, a lower long-term load deflection, and a higher rate of increase in long-term compressive stress in the bottom reinforcement compared to steel tendons. Opposite trends are seen when tendon relaxation is considered in numerical analysis.
- In the case of beams without external loads, increasing $\rho_s^{'}$ leads to an increase in long-term camber, a slight decrease in long-term axial shortening, a slight increase in long-term concrete compressive strain in the top fiber, and a decrease in long-term concrete compressive strain in the bottom fiber.
- Under service external loads, increasing $\rho_s^{'}$ reduces substantially the long-term

deflection, axial shortening and concrete compressive strain in the top fiber. A larger ρ_s' leads to a lower long-term tensile strain (for σ_{p0} = 800 MPa) or a higher long-term compressive strain (for σ_{p0} = 1200 MPa) of concrete in the bottom fiber.

- ACI 318-14 underestimates the effect of compressive reinforcing steel on the long-term deflection of prestressed concrete beams with unbonded CFRP tendons, especially at a high initial prestress level. ACI 318-14 substantially overestimates the time-dependent deflection for the initial prestress level of 60%.
- A modification of the ACI 318-14 equation is proposed to calculate the long-term deflection of prestressed concrete beams with FRP or steel tendons. By introducing the prestress-related parameters η_e, η_p and ξ_p, the proposed equation is shown to predict well the time-dependent deflection of prestressed concrete beams with unbonded CFRP tendons.

Acknowledgments

The work presented in this paper has been supported by the European Union's Horizon 2020 research and innovation program under the Marie Sklodowska-Curie grant agreement No. 751921.

References

[1] ACI committee 440. Prestressing concrete structures with FRP tendons. ACI 440.4R-04, Farmington Hills, MI; 2004.

[2] Lou T, Liu M, Lopes SMR, Lopes AV. Effect of bond on flexure of concrete beams prestressed with FRP tendons. Composite Structures 2017; 173: 168-176.

[3] Lou T, Lopes SMR, Lopes AV. A comparative study of continuous beams prestressed with bonded FRP and steel tendons. Composite Structures 2015; 124: 100-110.

[4] Atutis M, Valivonis J, Atutis E. Experimental study of concrete beams prestressed with basalt fiber reinforced polymers. Part I: Flexural behavior and serviceability. Composite Structures 2018; 183: 114-123.

[5] Lou T, Lopes SMR, Lopes AV. Response of continuous concrete beams internally prestressed with unbonded FRP and steel tendons. Composite Structures 2016; 154: 92-105.

[6] Au FTK, Du JS. Deformability of concrete beams with unbonded FRP tendons. Engineering Structures 2008; 30: 3764-3770.

[7] Heo S, Shin S, Lee C. Flexural behavior of concrete beams internally prestressed with unbonded carbon-fiber-reinforced polymer tendons. ASCE Journal of Composites for Construction 2013; 17(2): 167-175.

[8] Knight D, Visintin P, Oehlers DJ, Mohamed Ali MS. Simulating RC beams with unbonded FRP and steel prestressing tendons. Composites Part B: Engineering 2014; 60: 392-399.

[9] Ghallab A, Beeby AW. Factors affecting the external prestressing stress in externally strengthened prestressed concrete beams. Cement & Concrete Composites 2005; 27: 945-957.

[10] Bennitz A, Schmidt JW, Nilimaa J, Taljsten B, Goltermann P, Ravn DL. Reinforced concrete T-beams externally prestressed with unbonded carbon fiber-reinforced polymer tendons. ACI Structural Journal 2012; 109(4): 521-530.

[11] Lou T, Lopes SMR, Lopes AV. Factors affecting moment redistribution at ultimate in continuous beams prestressed with external CFRP tendons. Composites Part B: Engineering 2014; 66: 136-146.

[12] Wang X, Shi JZ, Wu G, Yang L, Wu ZS. Effectiveness of basalt FRP tendons for strengthening of RC beams through the external prestressing technique. Engineering Structures 2015; 101: 34-44.

[13] Lou T, Lopes SMR, Lopes AV. Effect of linear transformation on nonlinear behavior of continuous prestressed beams with external FRP cables. Engineering Structures 2017; 147: 410-424.

[14] Saadatmanesh H, Tannous FE. Relaxation, creep, and fatigue behavior of carbon fiber reinforced plastic tendons. ACI Materials Journal 1999; 96(2): 143-153.

[15] Saadatmanesh H, Tannous FE. Long-term behavior of aramid fiber-reinforced plastic (AFRP) tendons. ACI Materials Journal 1999; 96(3): 291-299.

[16] Rodriguez-Gutierrez JA, Aristizabal-Ochoa JD. Short- and long-term deflections in reinforced, prestressed, and composite concrete beams. ASCE Journal of Structural Engineering 2007; 133(4): 495-506.

[17] Au FTK, Si XT. Accurate time-dependent analysis of concrete bridges considering concrete creep, concrete shrinkage and cable relaxation. Engineering Structures 2011; 33: 118-126.

[18] Lou T, Lopes SMR, Lopes AV. A finite element model to simulate long-term behavior of prestressed concrete girders. Finite Elements in Analysis and Design 2014; 81: 48-56.

[19] Xue W, Liu T, Zeng M. Prediction of long-term deflections for high-speed railway prestressed concrete beams. ACI Structural Journal 2016; 113(4): 769-778.

[20] Huang H, Huang SS, Pilakoutas K. Modeling for assessment of long-term behavior of prestressed concrete box-girder bridges. ASCE Journal of Bridge Engineering 2018; 23(3): 04018002.

[21] Pisani MA. Long-term behaviour of beams prestressed with aramid fibre cables Part 1: a general method. Engineering Structures 2000; 22: 1641-1650.

[22] Pisani MA. Long-term behaviour of beams prestressed with aramid fibre cables Part 2: an approximate solution. Engineering Structures 2000; 22: 1651-1660.

[23] Lou T, Lopes SMR, Lopes AV. Time-dependent behavior of concrete beams prestressed with bonded AFRP tendons. Composites Part B: Engineering 2016; 97: 1-8.

[24] Youakim SA, Karbhari VM. An approach to determine long-term behavior of concrete members prestressed with FRP tendons. Construction and Building Materials 2007; 21: 1052-1060.

[25] ACI Committee 318. Building code requirements for structural concrete (ACI 318-14) and commentary (ACI 318R-14). American Concrete Institute, Farmington Hills, MI; 2014.

[26] Lou T, Lopes SMR, Lopes AV. Nonlinear and time-dependent analysis of continuous unbonded prestressed concrete beams. Computers & Structures 2013; 119: 166-176.

[27] Zienkiewicz OC, Watson M. Some creep effects in stress analysis with particular reference to concrete pressure vessels. Nuclear Engineering and Design 1966; 4(4): 406-412.

[28] Kwak HG, Kim JK. Time-dependent analysis of RC frame structures considering construction sequences. Building and Environment 2006; 41(10): 1423-1434.

[29] Norachan P, Kim KD, Onate E. Analysis of segmentally constructed prestressed concrete bridges using hexahedral elements with realistic tendon profiles. ASCE Journal of Structural Engineering 2014; 140(6): 04014028.

[30] Kang YJ, Scordelis AC. Nonlinear analysis of prestressed concrete frames. ASCE Journal of the Structural Division 1980; 106(ST2): 445-462.

[31] Magura DD, Sozen MA, Siess CP. A study of stress relaxation in prestressing reinforcement. PCI Journal 1964; 9(2): 13-57.

[32] Breckenridge RA, Bugg SL. Effects of long-time loads on prestressed concrete beams. PCI Journal 1964; 9(6): 75-89.

[33] Zhu BF. The finite element method theory and application. 3rd Edition, China Water Power Press, Beijing; 2009. (in Chinese)

[34] Ghali A, Favre R, Elbadry M. Concrete structures: stresses and deformation. 3rd Edition, Spon Press, London; 2002.

Table 1 Mechanical properties of CFRP and steel tendons.

Tendon	σ_{pu} (MPa)	f_{py} (MPa)	E_p (GPa)	ε_{pu} (%)
CFRP	1999.2	-	149.6	1.34
Steel	1860	1674	195	> 3.5

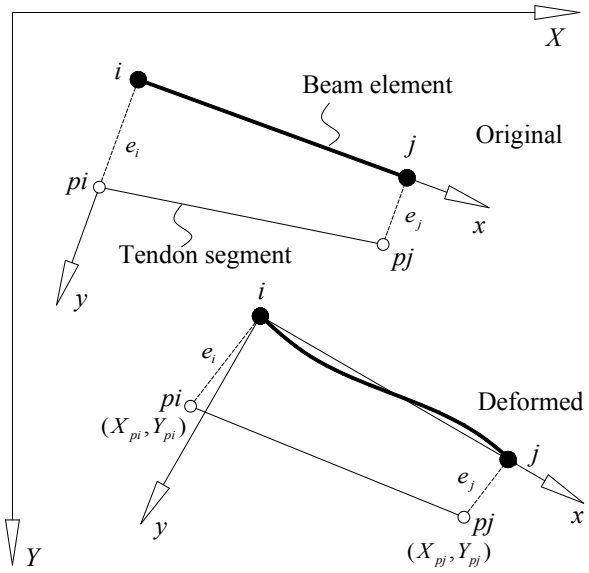

Fig. 1. Beam element and tendon segment before and after deformation

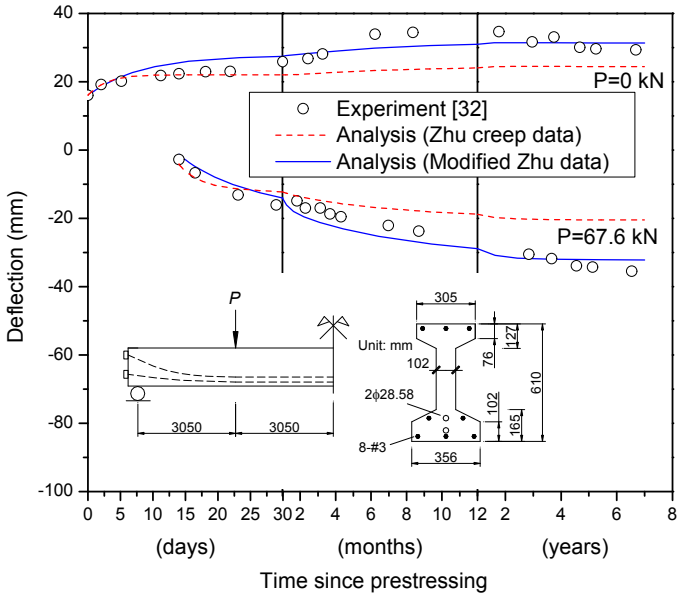

Fig. 2. Comparison of predicted long-term deflections with experimental data for unbonded prestessed concrete beam specimens.

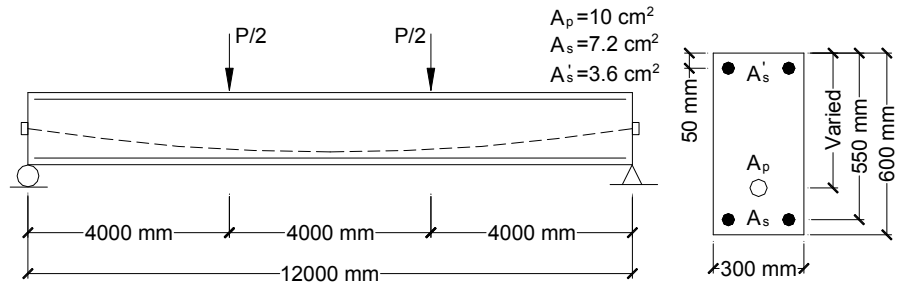

(a)

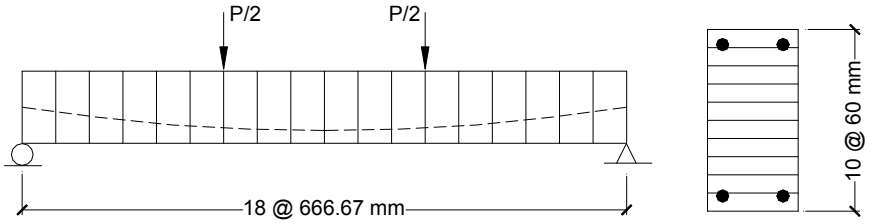

(b)

Fig. 3. Unbonded prestressed concrete beams for numerical investigation and the finite element model. (a) Beam details; (b) Finite element model.

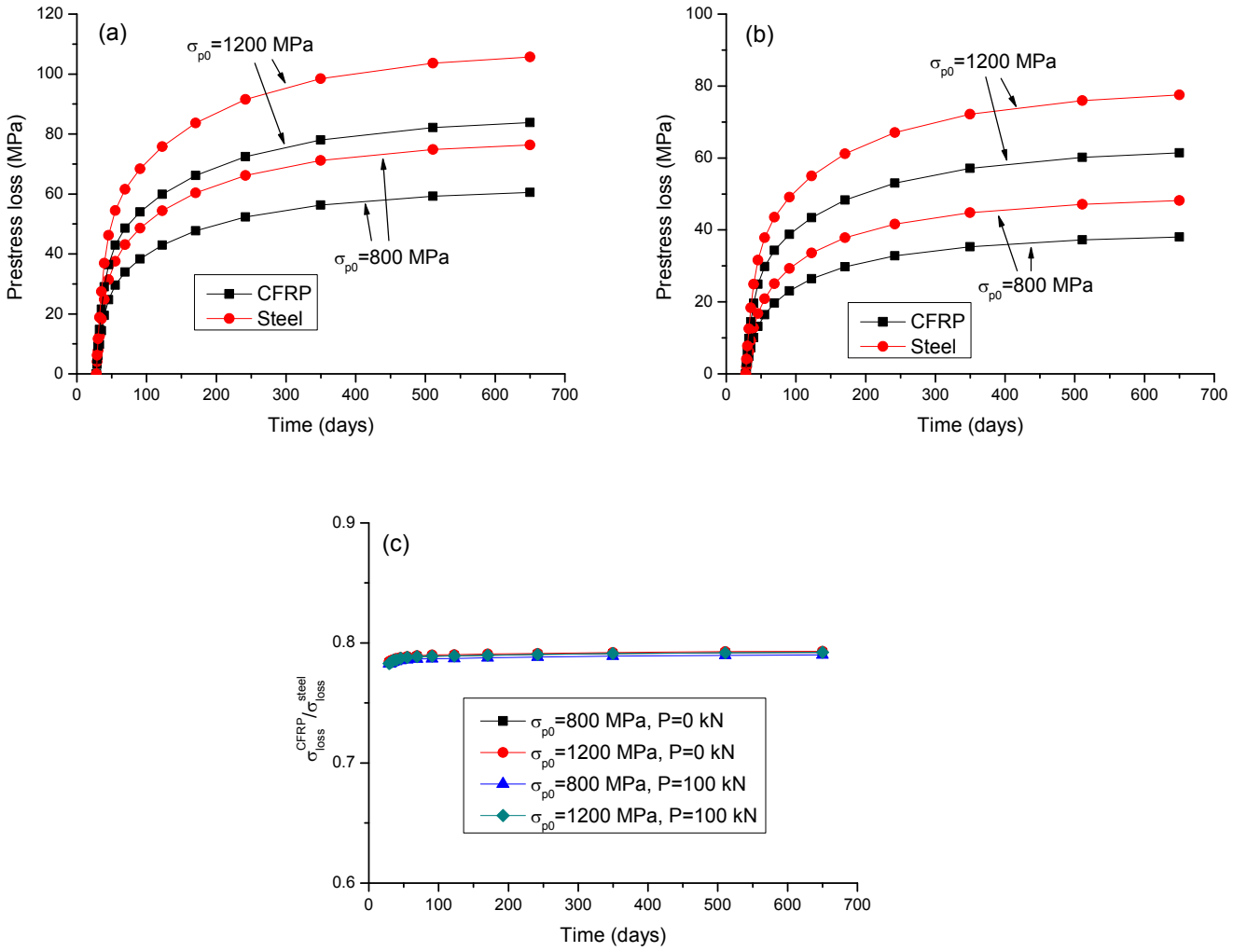

Fig. 4. Long-term prestress loss in unbonded CFRP and steel tendons caused by concrete creep and shrinkage. (a) Beams without external loads (P = 0 kN); (b) Beams with service external loads (P = 100 kN); (c) Ratio of prestress loss in CFRP tendons to that in steel ones.

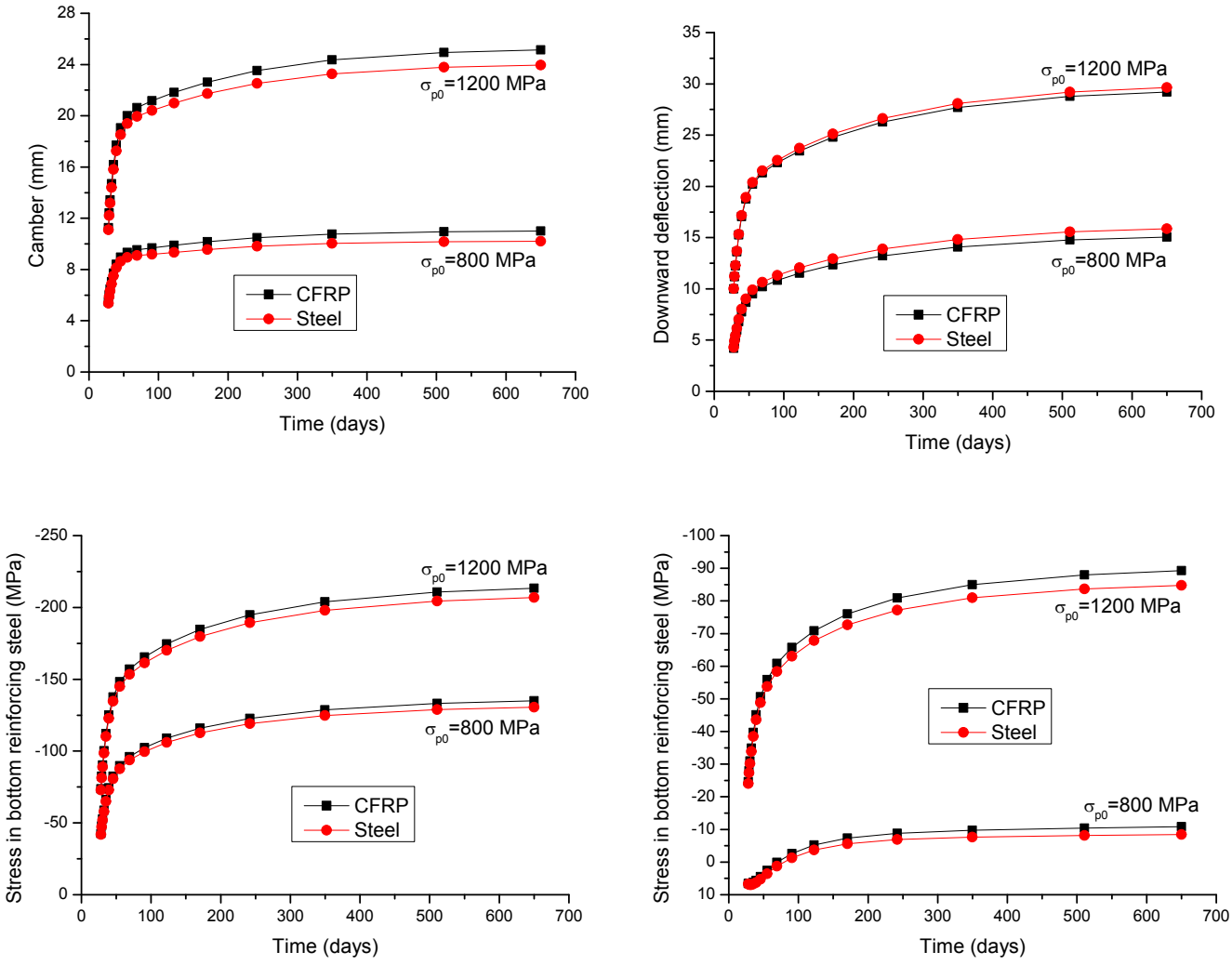

(a) (b)

Fig. 5. Long-term deflection and stress in bottom reinforcing steel caused by concrete creep and shrinkage. (a) Beams without external loads (P = 0 kN); (b) Beams with service external loads (P = 100 kN).

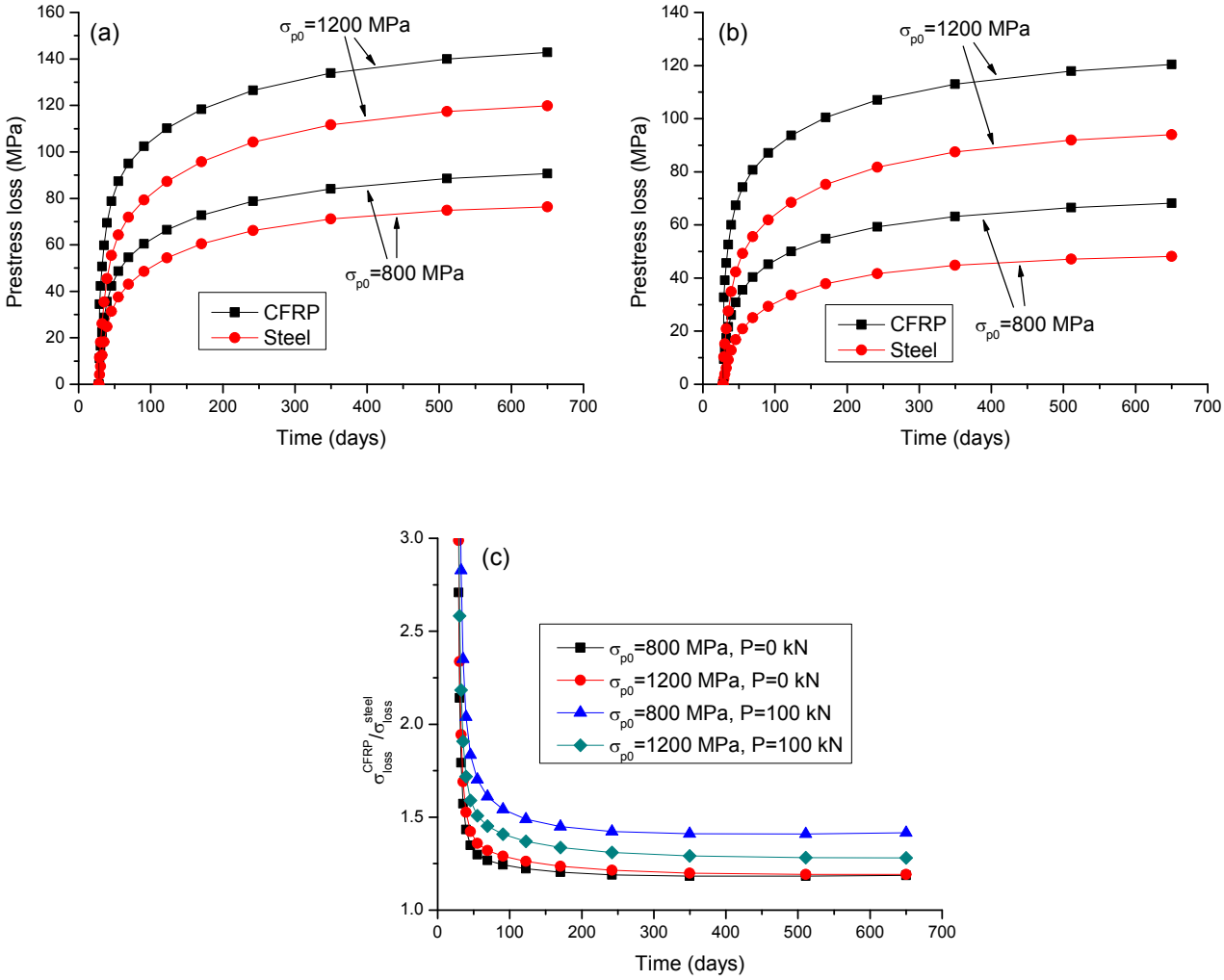

Fig. 6. Long-term prestress loss in unbonded CFRP and steel tendons caused by concrete creep, shrinkage and tendon relaxation. (a) Beams without external loads (P = 0 kN); (b) Beams with service external loads (P = 100 kN); (c) Ratio of prestress loss in CFRP tendons to that in steel ones.

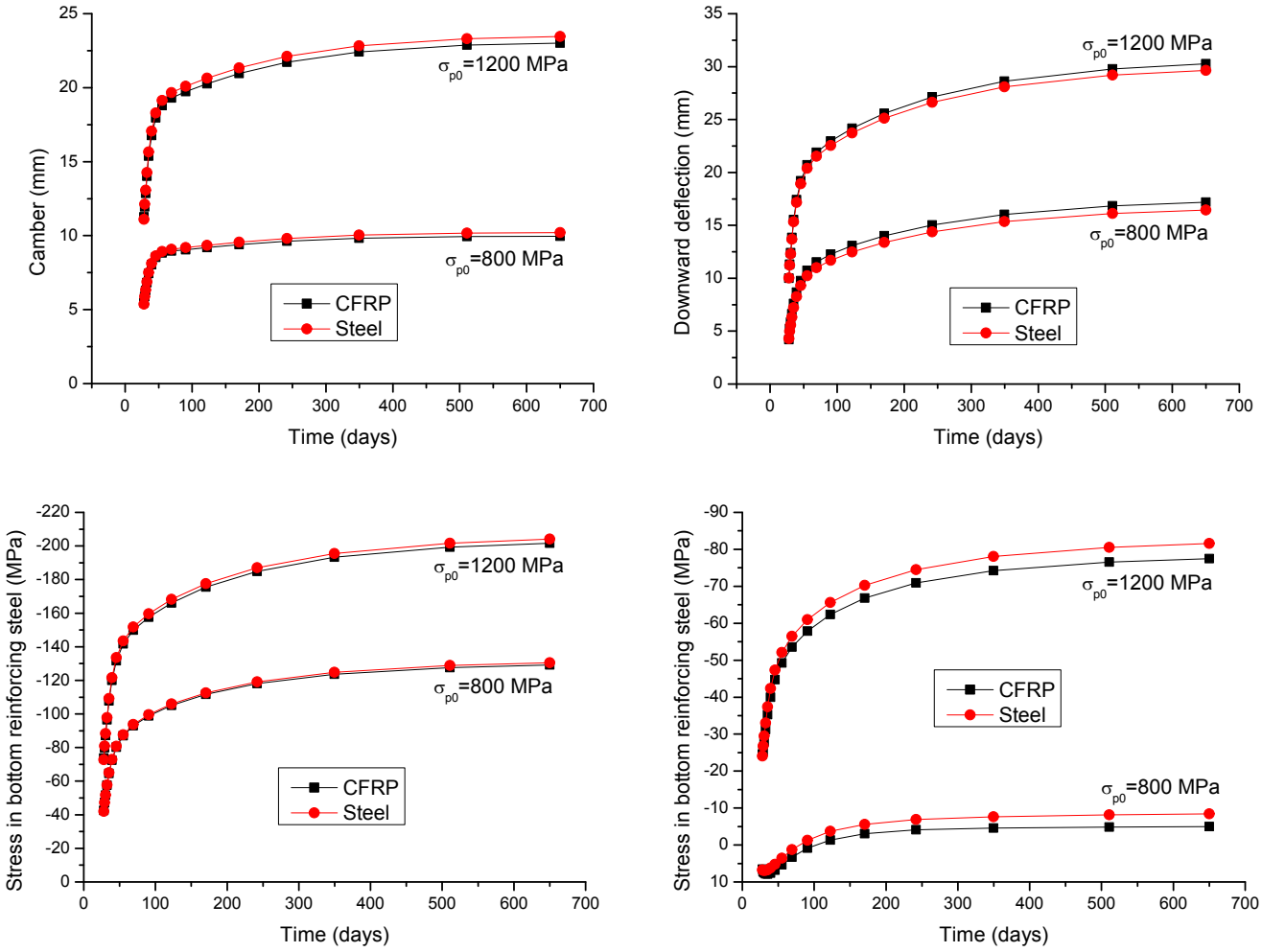

(a) (b)

Fig. 7. Long-term deflection and stress in bottom reinforcing steel caused by concrete creep, shrinkage and tendon relaxation. (a) Beams without external loads (P = 0 kN); (b) Beams with service external loads (P = 100 kN).

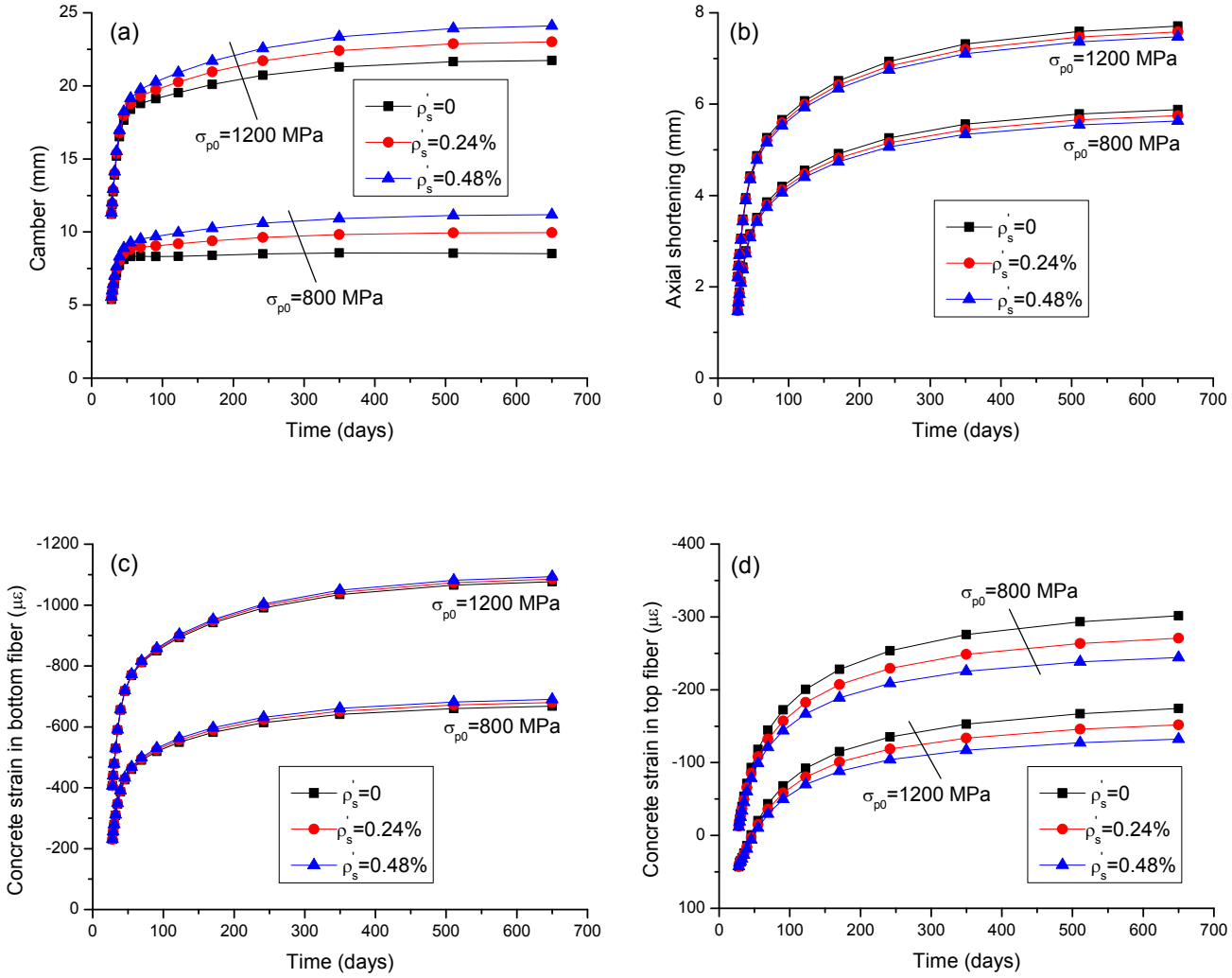

Fig. 8. Effect of ρ_s' on the long-term performance of unbonded CFRP tendon beams without external loads (P = 0 kN). (a) Camber; (b) Axial shortening; (c) Concrete strain in bottom fiber; (d) Concrete strain in top fiber.

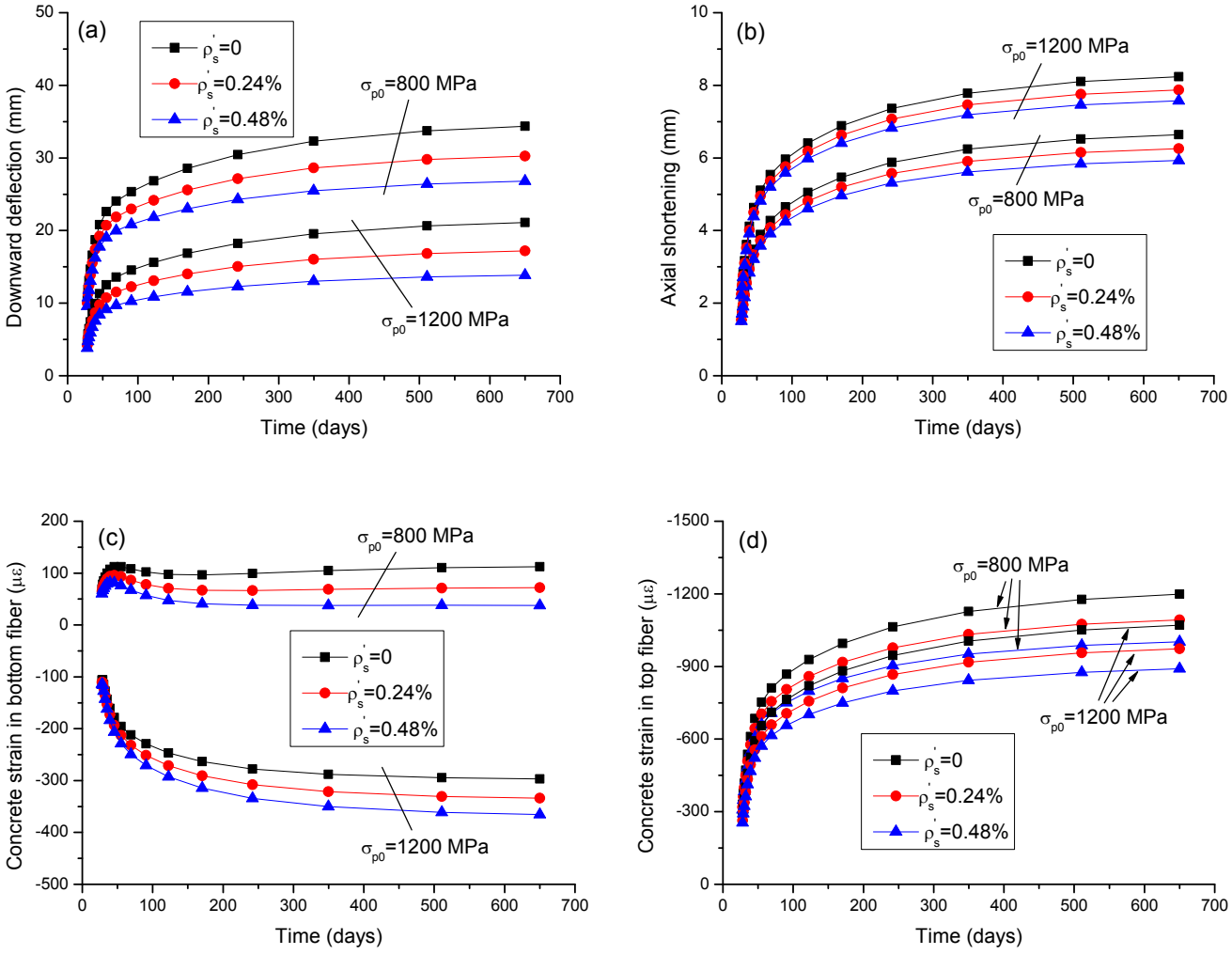

Fig. 9. Effect of ρ_s' on the long-term performance of unbonded CFRP tendon beams with service external loads (P = 100 kN). (a) Deflection; (b) Axial shortening; (c) Concrete strain in bottom fiber; (d) Concrete strain in top fiber.

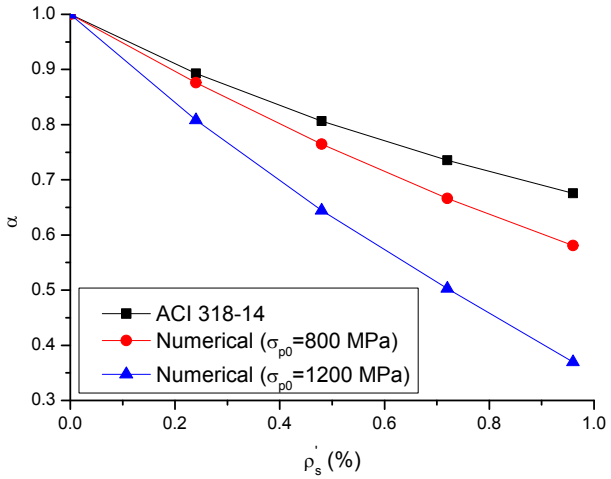

Fig. 10. Variation of α with ρ_s' according to ACI 318-14 and numerical simulations for 12-month loading.

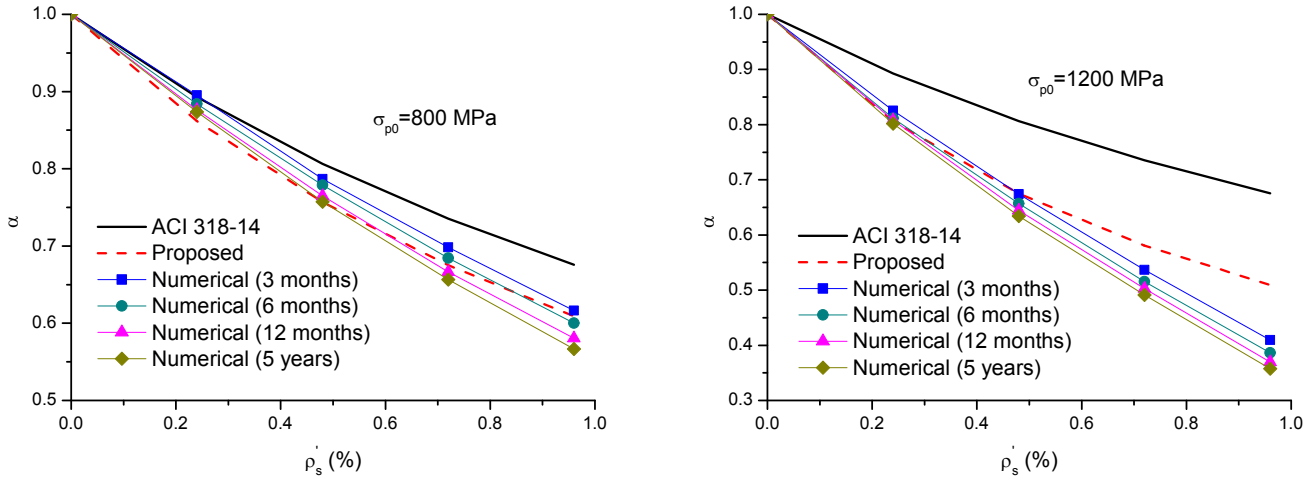

Fig. 11. Variation of α with ρ_s' according to ACI 318-14, the proposed equation and numerical simulations for different durations of loading and levels of initial prestress.

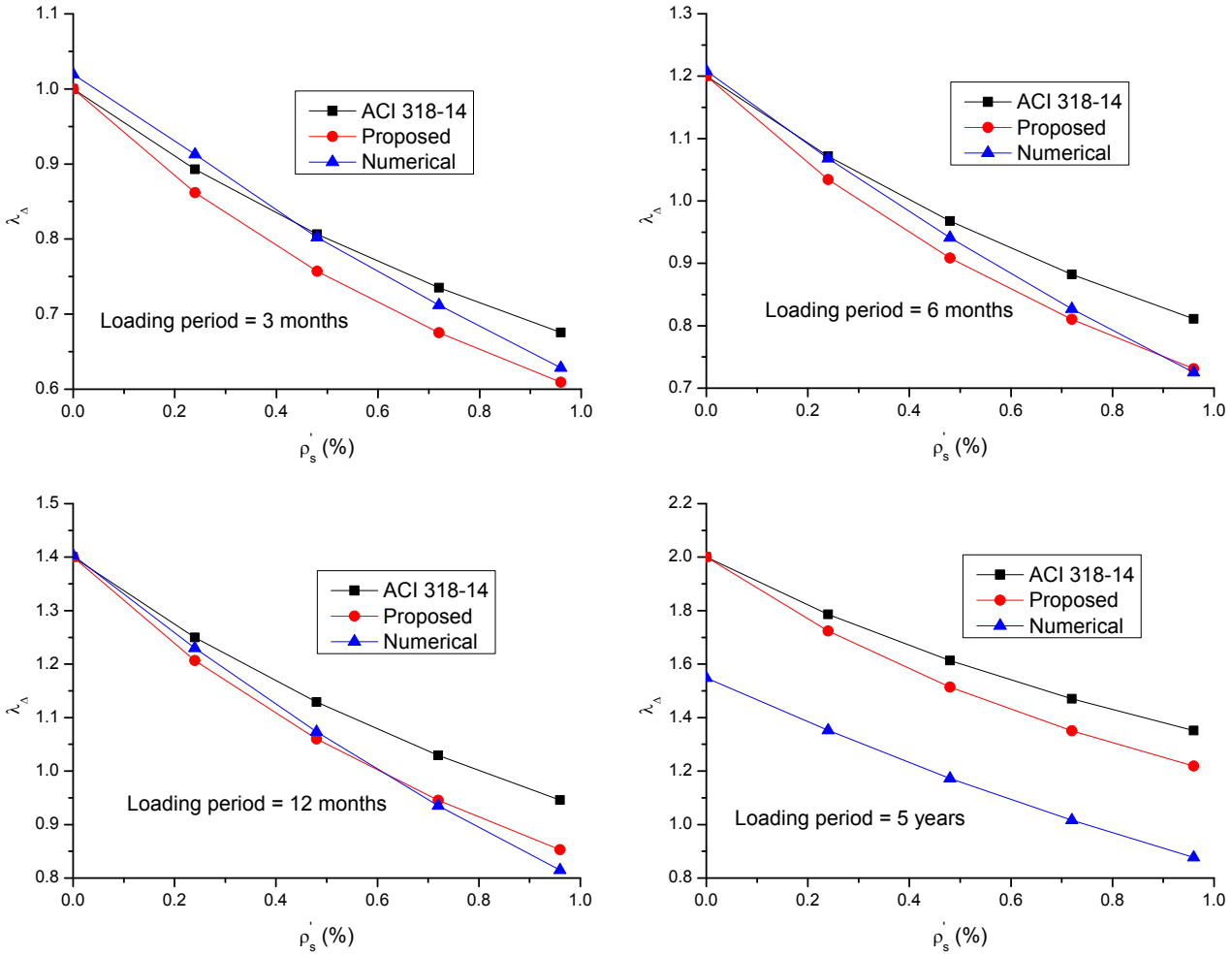

Fig. 12. Variation of λ_Δ with ρ_s' according to ACI 318-14, the proposed equation and numerical simulations for initial prestress of 800 MPa.

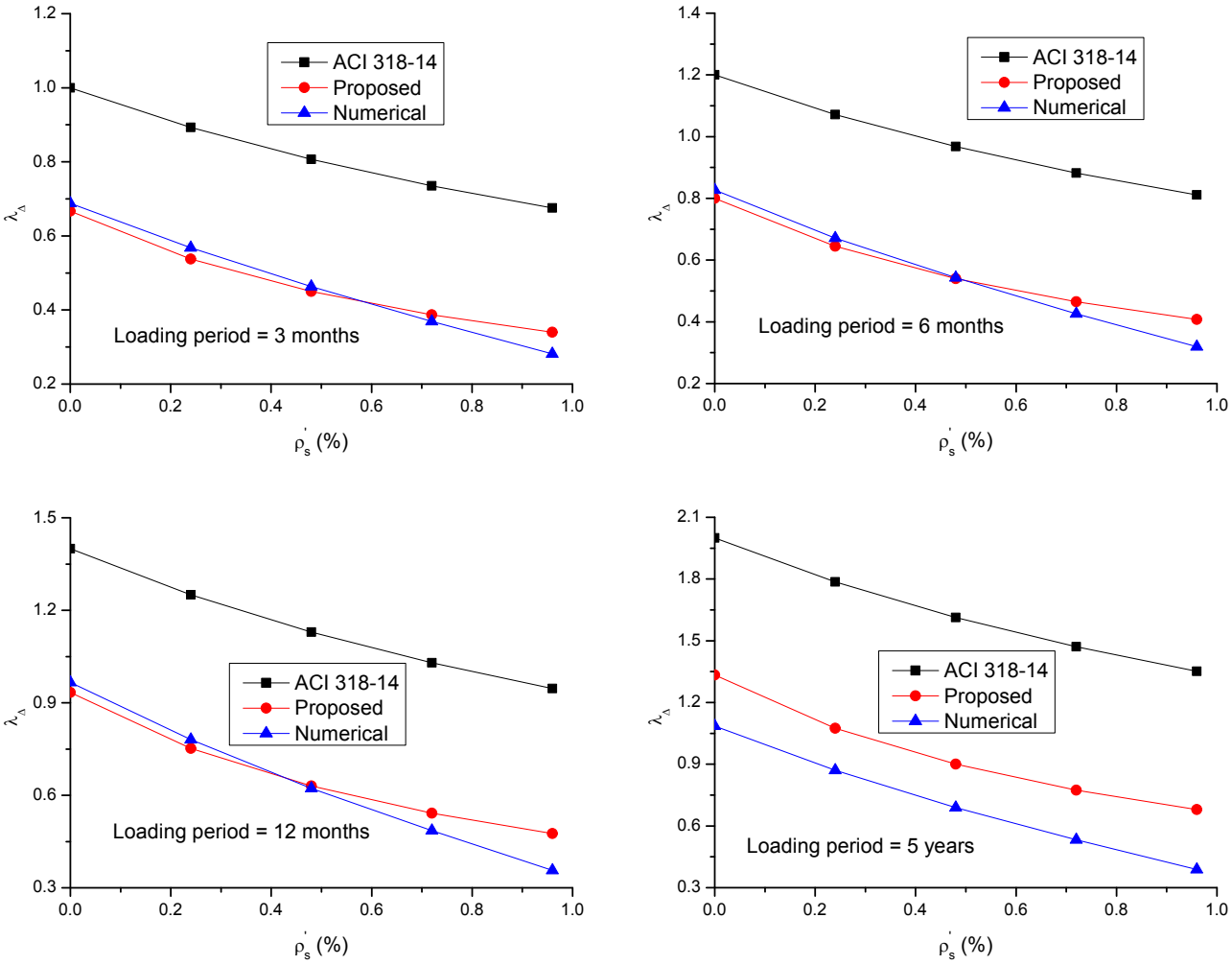

Fig. 13. Variation of λ_Δ with ρ_s' according to ACI 318-14, the proposed equation and numerical simulations for initial prestress of 1200 MPa.

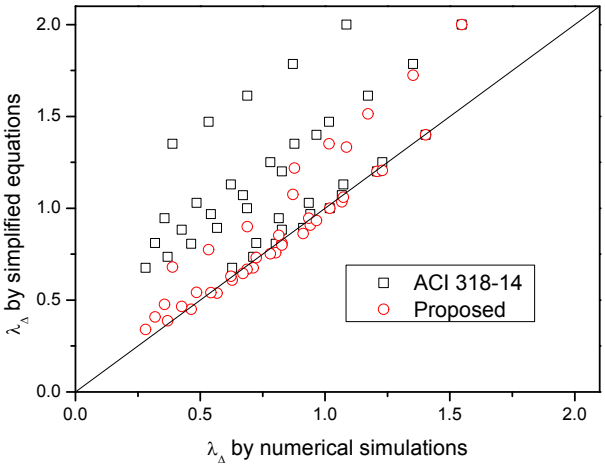

Fig. 14. Correlation of λ_{Δ} values predicted by simplified equations and numerical simulations.